DOI: 10.1002/ejic.200800121

Reactions of $[Hg(Tab)_2](PF_6)_2$ [Tab = 4-(trimethylammonio)benzenethiolate] with NaX (X = Cl, NO_2, NO_3): Isolation and Structural Characterization of a Series of Mono- and Binuclear Hg/Tab/X Compounds

Xiao-Yan Tang,[a] Jin-Xiang Chen,[a] Guang-Fei Liu,[a] Zhi-Gang Ren,[a] Yong Zhang,[a] and Jian-Ping Lang*[a,b]

Keywords: Mercury / S ligands / Bridging ligands

The complex $[Hg(Tab)_2](PF_6)_2$ [Tab = 4-(trimethylammonio)-benzenethiolate] (**1**) reacts with one or two equivalents of NaCl to afford the mononuclear complex $[Hg(Tab)_2Cl](PF_6)$ (**2**) and the dinuclear complex $[\{Hg(\mu\text{-}Tab)(Tab)Cl\}_2]Cl_2\cdot H_2O$ (**3**·H_2O), respectively. Similar reactions of **1** with NaCl and NaX (molar ratio = 1:1) produce the dinuclear species $[\{Hg(\mu\text{-}Tab)(Tab)Cl\}_2]X_2$ [X = NO_2 (**4**), NO_3 (**5**)], while those with $NaNO_2$ or $NaNO_3$ give rise to $[\{Hg(\mu\text{-}Tab)(Tab)X\}_2]X_2$ [X = NO_2 (**6**), NO_3 (**7**)]. Complexes **2**–**7** have been characterised by elemental analysis, IR, UV/Vis, and ^1H NMR spectroscopy, and X-ray crystallography. The Hg atom of the $[Hg(Tab)_2Cl]^+$ cation in **2** adopts a T-shaped coordination geometry. Two $[Hg(Tab)_2Cl]^+$ cations in **3**·H_2O, **4**, and **5** are linked by a pair of weak Hg–S bonds to form a dimeric $[Hg(\mu\text{-}Tab)(Tab)Cl]_2^{2+}$ dication, and the centrosymmetric $[Hg(\mu\text{-}Tab)(Tab)X]_2^{2+}$ dication in **6** and **7** consists of two $[Hg(Tab)_2X]^+$ cations linked by a couple of weak Hg–S bonds. The hydrogen-bonding interactions in **2**–**7** lead to the formation of interesting 2D (**5**, **7**) or 3D (**2**–**4**, **6**) hydrogen-bonded networks.

Introduction

The coordination chemistry of mercury thiolate complexes has attracted much interest in the past few decades because of their relation to biochemistry and toxicology.[1,2] A large number of structural studies have provided insights into the binding of mercury to metallothioneins (MTs)[3,4] and linear $\{Hg(S\text{-}Cys)_2\}$, trigonal $\{Hg(S\text{-}Cys)_3\}$, and tetrahedral $\{Hg(S\text{-}Cys)_4\}$ coordination geometries have been proposed for various Hg-MTs such as Hg_7-MT, Hg_{12}-MT, and Hg_{18}-MT.[5] From a structural point of view, the two- or three-coordinate Hg^{II} center in these Hg-MTs is unsaturated and may show potential reactivity toward other donor ligands, especially naturally occurring inorganic species like halide, nitrite, and nitrate anions. Such reactions may be important for the formation and stabilization of certain Hg-MTs. For instance, the formation of Hg_{18}-MT has been shown to be highly dependent on the presence of Cl^- ions and a pH below 6.[6] However, to the best of our knowledge, few reports have discussed the reactivities of the Hg^{II} centers in Hg-MTs toward halide, nitrite, and nitrate anions. This is probably due to the low solubility of most Hg/thiolate complexes in common solvents and the limited number of suitable model complexes that can be used to mimic the Hg^{II} centers in Hg-MTs.

We have recently become interested in the preparation of a series of metal thiolate complexes from the zwitterionic thiolate ligand $(TabH)PF_6$ [Tab = 4-(trimethylammonio)-benzenethiolate].[7] Among them, $[Hg(Tab)_2](PF_6)_2$ (**1**) is likely to be a potential precursor to mimic the reactivity of the Hg^{II} centers in Hg-MTs because its central Hg atom adopts an unsaturated two-coordinate linear geometry and can react with donor ligands (e.g. Tab, SCN^-, I^-).[7d] However, do naturally occurring inorganic anions such as Cl^-, NO_2^-, and NO_3^- react with the Hg^{II} center of **1**? Does the introduction of these anions change the structure of **1**? What is the role of these anions in the formation of the resulting hydrogen-bonded structures? With these questions in mind, we decided to study the reactions of **1** with NaCl, $NaNO_2$, and $NaNO_3$ and obtained the Hg/Tab/X (X = Cl^-, NO_2^-, or NO_3^-) complexes $[Hg(Tab)_2Cl](PF_6)$ (**2**), $[Hg(\mu\text{-}Tab)(Tab)Cl]_2Cl_2\cdot H_2O$ (**3**·H_2O), $[Hg(\mu\text{-}Tab)(Tab)Cl]_2(NO_2)_2$ (**4**), $[Hg(\mu\text{-}Tab)(Tab)Cl]_2(NO_3)_2$ (**5**), $[Hg(\mu\text{-}Tab)(Tab)(NO_2)]_2(NO_2)_2$ (**6**), and $[Hg(\mu\text{-}Tab)(Tab)(NO_3)]_2(NO_3)_2$ (**7**). Herein we discuss these reactions and the isolation and structural characterization of **2**–**7** in detail.

[a] Key Laboratory of Organic Synthesis of Jiangsu province, School of Chemistry and Chemical Engineering, Suzhou University,
Suzhou 215123, Jiangsu, People's Republic of China
Fax: +86-512-6588-0089
E-mail: jplang@suda.edu.cn
[b] State Key Laboratory of Coordination Chemistry, Nanjing University,
Nanjing 210093, Jiangsu, People's Republic of China
Supporting information for this article is available on the WWW under http://www.eurjic.org or from the author.

Results and Discussion

The reactions of **1** with three commonly encountered inorganic salts (NaCl, $NaNO_2$ and $NaNO_3$) occur in a straightforward manner, although some of them depend strongly on the ratio between **1** and these salts. Thus, treatment of **1** with an equimolar amount of NaCl in MeOH/H_2O afforded the mononuclear complex **2** (Scheme 1), whereas the treatment of **1** with two equivalents of NaCl, or of **2** with one or more equivalents of NaCl, did not produce the expected neutral molecule $[Hg(Tab)_2Cl_2]$ but instead gave rise to the dimeric cationic complex **3**·H_2O in relatively high yield. The treatment of **1** with equimolar amounts of NaCl and NaX formed similar dinuclear cationic species $[\{Hg(\mu\text{-}Tab)(Tab)Cl\}_2]X_2$ in 79% yield for X = NO_2 (**4**) and 74% yield for X = NO_2 (**5**). Analogous reactions of **1** with two equivalents of $NaNO_2$ or $NaNO_3$ in dmf/H_2O produced the dimeric complexes $[\{Hg(\mu\text{-}Tab)(Tab)X\}_2]X_2$ in 72% yield for X = NO_2 (**6**) and 73% yield for X = NO_3 (**7**). Similar reactions with different reagent ratios (1:1 to 1:4) yielded the same products.

Compounds **2**–**7** are stable toward oxygen and moisture and are soluble in MeCN, DMSO, and dmf but not in CH_2Cl_2, MeOH, benzene, and H_2O. The elemental analyses of **2**–**7** are consistent with their chemical formula. The ^1H NMR spectra of **2**–**7** in DMSO at room temperature show a multiplet for the Ph groups at δ = 7.37–7.75 ppm and a singlet for the NMe_3 protons at about δ = 3.38 ppm. The IR spectrum of **2** shows characteristic P–F stretching vibrations for the PF_6^- anion at $\tilde{\nu}$ = 839 and 558 cm^{-1}. The IR spectra of **4** and **6** feature absorption bands arising from the nitrite anions. As will be described later in this paper, complex **6** contains two different types of nitrites, namely a discrete nitrite anion and a nitrite that is weakly chelating to the Hg atoms. The nitrite of **4** is of the former type and acts as a counteranion. The strong bands at 1273 and 1219 cm^{-1} in the IR spectrum of **4** can be unequivocally assigned to the asymmetric and symmetric N–O stretching vibrational modes, respectively.[8a] In contrast, the IR spectrum of **6** shows two strong and broad peaks at 1270 and 1210 cm^{-1}, which are somewhat broader than the corresponding bands for **4**. We therefore assume that the asymmetric and symmetric N–O stretching vibrations of the discrete nitrite overlap with those of the chelating nitrite. Similarly, the relatively broad band at 1382 cm^{-1} in the IR spectrum of **5** can be assigned to the asymmetric N–O stretching vibration mode of the nitrate counterion,[8b] and the peak at 1324 cm^{-1} in the IR spectrum of **7** can be assigned to one of the two peaks arising from the splitting of the asymmetric N–O stretching mode of the Hg-bound nitrate. The other peak may overlap with the signal of the discrete nitrate anion, thereby leading to a relatively broad peak at 1384 cm^{-1}.

As shown in Figure 1, the electronic spectra of **1**–**7** and the free Tab ligand in MeCN exhibit a strong and broad absorption ranging from 258 to 269 nm with a long absorption tail to around 400 nm. The peaks observed in the spectra of **2**–**7** are blue-shifted with respect to the broad absorption band at 314 nm for the Tab ligand in MeCN, which may be ascribed to a ligand(Tab)-to-metal charge transfer (LMCT).[9] It should be noted that mercury(II) thiolates with a distorted tetrahedral geometry usually show low-en-

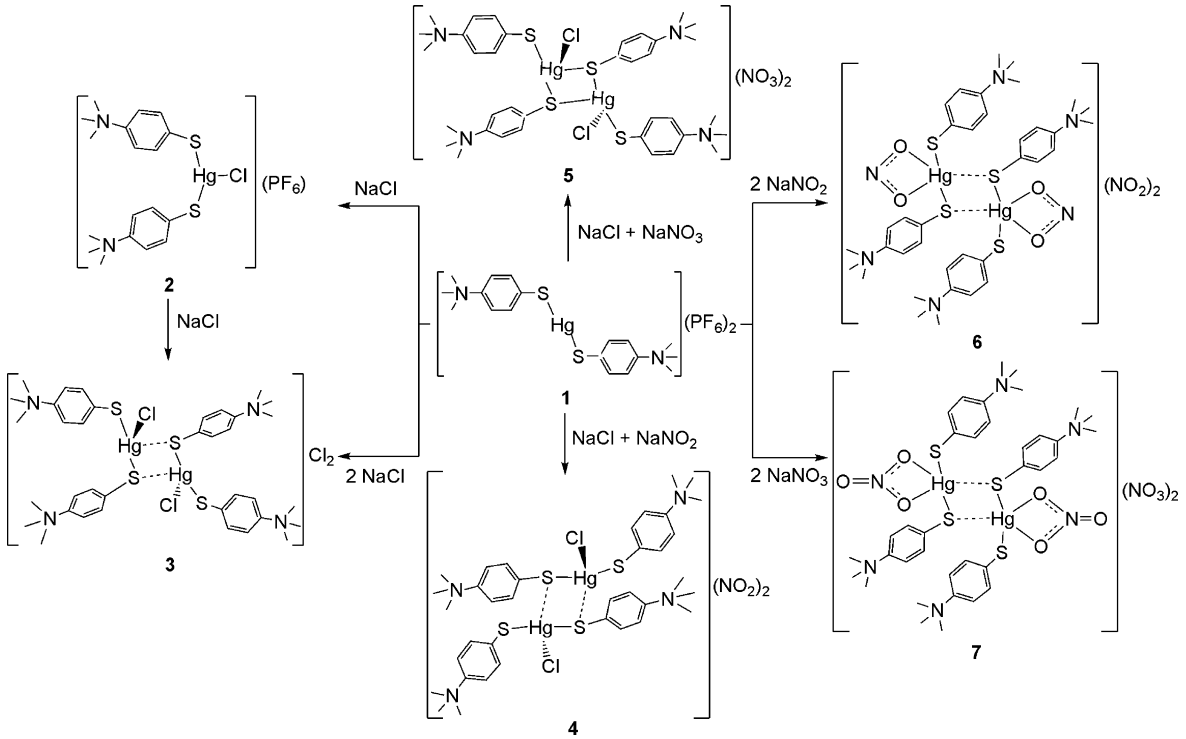

Scheme 1. Reactions of $[Hg(Tab)_2](PF_6)_2$ (**1**) with NaCl, $NaNO_2$, and $NaNO_3$.

ergy charge-transfer bands at 280–310 nm, as observed in $[Hg(SR)_2]$ (R = Et and *i*Pr),[5c] mercury plastocyanin,[10] and two types of metallothionein.[11] This difference might be due to the presence of one or two additional Hg–Cl (or O) bonds.

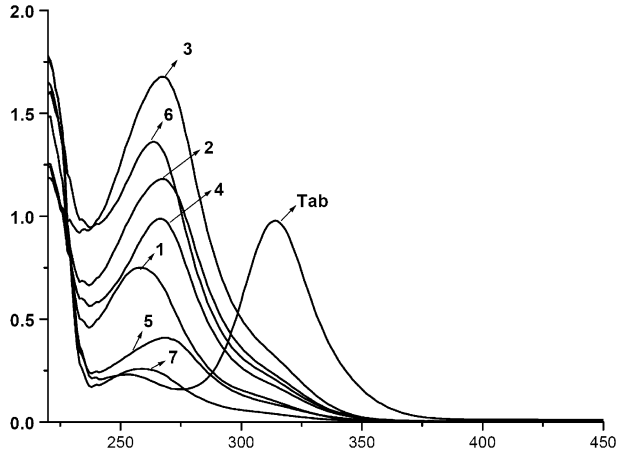

Figure 1. Electronic spectra of **1**–**7** and Tab in MeCN with a 1-mm optical path length.

The peaks in the spectra of **2**–**7** are slightly red-shifted relative to the peaks of **1** and other Hg/Tab compounds. This may be ascribed to the fact that the structures of **2**–**7** roughly retain the $[Hg(Tab)_2]^{2+}$ species of **1**, although the related Hg atoms have somewhat different coordination geometries when they bind other donor atoms.

Compound **2** crystallizes in the monoclinic space group $P2_1/c$ and its asymmetric unit contains one $[Hg(Tab)_2Cl]^+$ cation and one PF_6^- anion. The Hg(1) atom in the $[Hg(Tab)_2Cl]^+$ cation is coordinated by one Cl atom and two S atoms from two Tab ligands to form an approximate T-shaped coordination geometry [S(1)–Hg(1)–S(2) 169.83(6)°; Figure 2] similar to those found in Hg^{II}/amino acid complexes such as the L-cysteine complex $[Hg\{L\text{-}SCH_2CH(NH_3)COO\}\{L\text{-}SCH_2CH(NH_3)COOH\}]Cl$[12] and the penicillamine complex $[Hg\{SCMe_2CH(NH_3)COOH\}_2Cl]Cl$.[13]

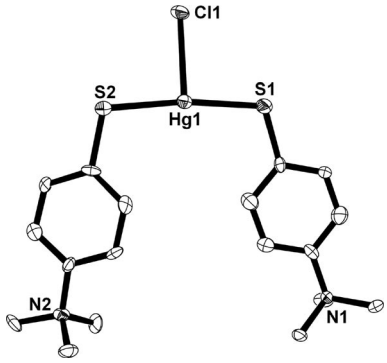

Figure 2. Perspective view of the $[Hg(Tab)_2Cl]^+$ cation of **2** showing 50% thermal ellipsoids. All hydrogen atoms have been omitted for clarity.

It should be noted that the two $^-SC_6H_4NMe_3^+$ groups in **2** are oriented in the same direction compared with those in **1**, which suggests that one of the two $^-SC_6H_4NMe_3^+$ groups of **1** is rotated around the S–Hg–S line by about 180° during the reaction. The mean Hg–S bond length [2.3576(17) Å] is slightly longer than those of **1** [2.331(2) Å][7d] and $[Hg(SCMe_2CH(NH_3)COOH)_2Cl]Cl$ [2.346(3) Å],[13] but shorter than that observed in $[Hg(C_3H_2NS)_2Cl_2]$ [2.532(4) Å; C_3H_2NS = *N*,*N*-dimethylthioformamide].[14] The Hg(1)–Cl(1) bond length [2.7332(15) Å] is shorter than that in $[Hg(SCMe_2CH(NH_3)COOH)_2Cl]Cl$ [2.850(5) Å], but much longer than those of $[Hg(C_5H_{11}NOS)Cl_2]$ [2.422(3) Å; $C_5H_{11}NOS$ = *N*,*N*-dimethyl-*o*-ethylthiocarbamato-S][15] and $[Hg\{SC(NH_2)_2\}_2Cl]Cl$ (2.570 Å).[16] The distance between Hg in one cation and S in the adjacent cation (4.133 Å) precludes any Hg and S interaction. The Hg···Hg separation between two neighboring cations is 5.161 Å.

There are two intramolecular hydrogen-bonding interactions between F atoms of PF_6^- anions and the H atoms of the methyl groups with C(17) and C(18) [C(17)···F(6) 3.161(7), C(18)···F(2) 3.457(7) Å], and two intermolecular H-bonding interactions between the terminal Cl(1) atom and the methyl group with C(16) [C(16)···Cl(1) ($-x$, $y - 1/2$, $-z + 3/2$) 3.714(6) Å] and between the F(4) atom of the PF_6^- anion and the methyl group with C(8) [C(8)···F(4) ($x - 1$, y, z) 3.389(7) Å] form a 2D layered network that extends in the *ab* plane. Each layer is further interconnected with adjacent layers via one intermolecular H-bonding interaction between the F(5) atom of the PF_6^- anion and the H atom of the phenyl group with C(2) [C(2)···F(5) ($x - 1$, $-y + 1/2$, $z + 1/2$) 3.418 Å], which leads to the formation of a 3D hydrogen-bonded structure (Figure 3).

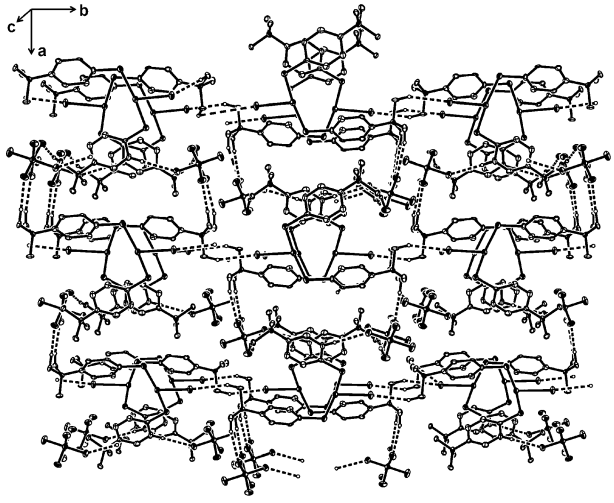

Figure 3. View of the three-dimensional hydrogen-bonded structure formed via H-bonding interactions in **2** looking down the *c* axis. All H atoms except those related to H-bonding interactions have been omitted for clarity.

Compound **3**·H_2O crystallizes in the monoclinic space group *Pn* and the asymmetric unit consists of one $[Hg(\mu\text{-}Tab)(Tab)Cl]_2^{2+}$ dication, two Cl^- anions, and one water solvent molecule, whereas **4** and **5** crystallize in the monoclinic space group $P2_1/c$ (**4**) or $P2_1/n$ (**5**) and the asymmetric unit contains half of a $[Hg(\mu\text{-}Tab)(Tab)Cl]_2^{2+}$ dication and one

NO_2^- (**4**) or NO_3^- (**5**) anion. As the structures of the dications of **3**·H_2O, **4**, and **5** are quite similar, only the perspective view of the dication in **3**·H_2O is depicted in Figure 4. The $[Hg(\mu\text{-Tab})(Tab)Cl]_2^{2+}$ dication of **3**·H_2O consists of two $[Hg(Tab)_2Cl]^+$ cations that are linked by a pair of Hg–S bonds to form an asymmetrical Hg_2S_2 rhomb with two short and two longer bridging Hg–S bonds. There is no symmetry in the dication of **3**·H_2O, but those of **4** and **5** have a crystallographic inversion center at the center of the Hg_2S_2 rhomb. The two $^-SC_6H_4NMe_3^+$ groups of each $[Hg(Tab)_2Cl]^+$ cation in **3**·H_2O and **5** are oriented in the same direction as those of **1**, while those of **4** keep their original orientation. The dihedral angles between the two phenyl groups are 37.3° and 44.3° for **3**·H_2O, 51.0° for **4**, and 49.2° for **5**. Each Hg atom is coordinated by one Cl and three S atoms from one terminal and two bridging Tab ligands to form a highly distorted tetrahedral coordination geometry.

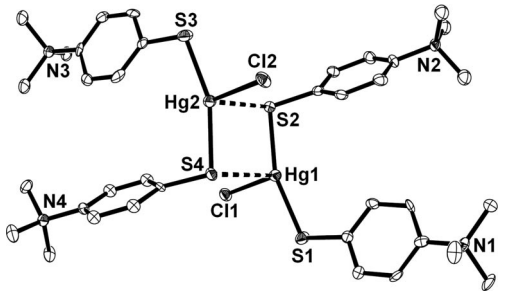

Figure 4. Perspective view of the $[Hg(\mu\text{-Tab})(Tab)Cl]_2^{2+}$ dication of **3**·H_2O showing the atom labeling scheme and 50% thermal ellipsoids.

The Hg···Hg contact in the dication [3.996(3) Å for **3**·H_2O, 4.094(5) Å for **4**, and 4.020(2) Å for **5**] is longer than those observed in $[Hg_2(Tab)_6]Y$ [3.637(2) Å for Y = $(PF_6)_4$; 3.592(2) Å for Y = $(PF_6)Cl_{11}$][7d] and $[Et_4N]_2[Hg_2(SMe)_6]$ [3.631(6) Å].[17] The mean terminal Hg–S bond length [2.3724(16) Å in **3**·H_2O, 2.314(2) Å in **4**, and 2.3363(16) Å in **5**; see Table 1] is shorter than those found in similar Hg^{II} dimeric structures such as $[Hg_2(Tab)_6]Y$ [2.4242(14) Å for Y = $(PF_6)_4$; 2.4310(13) Å for Y = $(PF_6)Cl_{11}$] and $[Et_4N]_2[Hg_2(SMe)_6]$ [2.456(2) Å], while the mean bridging Hg–S bond length [2.7496(16) Å in **3**·H_2O, 2.755(2) Å in **4**, and 2.693(16) Å in **5**] is similar to those in $[Hg_2(Tab)_6]Y$ [2.6895(13) Å for Y = $(PF_6)_4$; 2.6945(12) Å for Y = $(PF_6)Cl_{11}$] and $[Et_4N]_2[Hg_2(SMe)_6]$ [2.668(2) Å]. The mean Hg–Cl bond length in **3**·H_2O [2.6405(18) Å] is similar to that in **5** [2.643(15) Å] but somewhat shorter than those of **4** [2.789(3) Å] and **1** [2.7332(15) Å].

Table 1. Selected bond lengths [Å] and angles [°] for **2**–**7**.

Compound **2**			
Hg(1)–S(1)	2.3487(17)	Hg(1)–S(2)	2.3665(17)
Hg(1)–Cl(1)	2.7332(15)	S(1)–Hg(1)–S(2)	169.83(6)
S(1)–Hg(1)–Cl(1)	93.44(5)	S(2)–Hg(1)–Cl(1)	95.89(5)
Compound **3**			
Hg(1)–S(1)	2.3474(17)	Hg(2)–S(3)	2.3541(17)
Hg(1)–S(2)	2.3723(16)	Hg(2)–S(4)	2.3726(15)
Hg(1)–S(4)	3.1462(16)	Hg(2)–S(2)	3.1072(16)
Hg(1)–Cl(1)	2.6548(18)	Hg(2)–Cl(2)	2.6262(18)
S(1)–Hg(1)–S(2)	161.06(6)	S(3)–Hg(2)–S(4)	159.40(6)
S(1)–Hg(1)–Cl(1)	94.62(6)	S(2)–Hg(1)–Cl(1)	100.83(6)
S(3)–Hg(2)–Cl(2)	97.44(6)	S(4)–Hg(2)–Cl(2)	101.03(6)
Compound **4**			
Hg(1)–S(1)	2.297(3)	Hg(1)–S(2)	2.331(2)
Hg(1)–S(1A)	3.179(2)	Hg(1)–Cl(1)	2.789(3)
S(1)–Hg(1)–S(2)	159.65(9)	S(1)–Hg(1)–Cl(1)	111.50(8)
S(2)–Hg(1)–Cl(1)	88.25(9)		
Compound **5**			
Hg(1)–S(1)	2.3363(16)	Hg(1)–S(2A)	2.267(16)
Hg(1)–S(2)	3.118(3)	Hg(1)–Cl(1)	2.643(15)
S(1)–Hg(1)–S(2)	143.01(12)	S(1)–Hg(1)–Cl(1)	95.57(10)
S(2)–Hg(1)–Cl(1)	113.54(5)		
Compound **6**			
Hg(1)–S(1)	2.3458(12)	Hg(1)–S(2)	2.3598(12)
Hg(1)–O(1)	2.643(3)	Hg(1)–O(2)	2.683(9)
Hg(1)–S(2A)	3.222(3)	Hg(1A)–S(2)	3.222(3)
S(1)–Hg(1)–S(2)	164.41(4)		
Compound **7**			
Hg(1)–S(1)	2.3400(11)	Hg(1)–S(2)	2.3464(11)
Hg(1)–O(1)	2.714(3)	Hg(1)–O(2)	2.796(3)
Hg(1)–S(2A)	3.273(11)	Hg(1A)–S(2)	3.273(11)
S(1)–Hg(1)–S(2)	173.04(3)		

The hydrogen-bonding interactions in **3**·H_2O, **4**, and **5** are rather complicated. Thus, for **3**·H_2O there are five intramolecular H-bonding interactions between Cl(3) and the methyl group with C(7) [C(7)···Cl(3) 3.574(7) Å], Cl(4) and the H_2O molecule [O(1)···Cl(4) 3.035(5) Å] or the methyl group with C(7) [C(7)···Cl(4) 3.745(7) Å], and between the O atom of the H_2O molecule and the phenyl group with C(12) [C(12)···O(1) 3.373(8) Å] or the methyl group with C(16) [C(16)···O(1) 3.261(8) Å]. One intermolecular H-

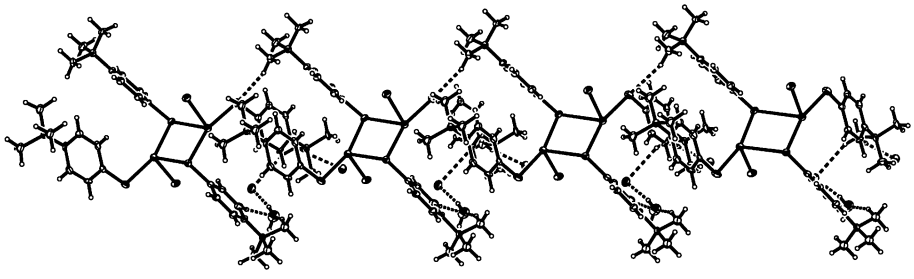

Figure 5. View of the chain structure of **3**·H_2O running along the *a* axis formed by H-bonding interactions.

bonding interaction between the S atom of the Tab ligand and the methyl group with C(36) [C(36)···S(1) (x + 1, y, z) 3.688(6) Å] produces a chain structure running along the *a* axis (Figure 5).

Each chain is further linked with neighboring chains via two intermolecular H-bonding interactions between Cl(4) and the methyl group with C(34) or C(35) [C(34)···Cl(4) (x + 1/2, –y + 2, z – 1/2) 3.674(7), C(35)···Cl(4) (x + 1/2, –y + 2, z – 1/2) 3.675(6) Å], which leads to a 2D hydrogen-bonded layer extending in the *ac* plane. Finally, adjacent layers are interconnected by a set of intermolecular H-bonding interactions between Cl(1), Cl(2), or Cl(3) and the phenyl group with C(3), C(23), or C(30) [C(3)···Cl(1) (–1/2 + x, 2 – y, 1/2 + z) 3.522(6), C(23)···Cl(2) (1/2 + x, 1 – y, –1/2 + z) 3.556(7), C(30)···Cl(3) (1 + x, y, –1 + z) 3.656(6) Å] and between Cl(1) or Cl(3) and the methyl group with C(18) or C(25) [C(18)···Cl(1) (–1/2 + x, 1 – y, 1/2 + z) 3.707(6), C(18)···Cl(3) (1/2 + x, 1 – y, –1/2 + z) 3.551(6), C(25)···Cl(3) (1 + x, y, –1 + z) 3.629(8) Å] to afford a 3D hydrogen-bonded structure (see Figure S3 in the Supporting Information).

For **4**, several intermolecular H-bonding interactions between Cl(1) and the methyl group with C(8) [C(8)···Cl(1) (3 – x, 1/2 + y, 3/2 – z) 3.689(9) Å] or the phenyl group with C(14) [C(14)···Cl(1) (–1 + x, 3/2 – y, –1/2 + z) 3.652(10) Å], between O(1) of the NO_2^- anion and the methyl groups with C(8) and C(16) [C(8)···O(1) (2 – x, 2 – y, 1 – z) 3.338(12), C(16)···O(1) (1 – x, 3/2 – y, –1/2 + z) 3.458(11) Å], and between O(2) of the NO_2^- anion and the phenyl groups with C(3) [C(3)···O(2) (1 + x, 3/2 – y, 1/2 + z) 3.332(11) Å] or the methyl groups with C(9) and C(16) [C(9)···O(2) (1 + x, 3/2 – y, 1/2 – z) 3.419(13), C(16)···O(2) (1 – x, –1/2 + y, 1/2 – z) 3.395(13) Å] afford a 2D hydrogen-bonded network extending in the *ab* plane (Figure 6). Neighboring layers are further connected by one intermolecular H-bonding interaction between S(2) and the methyl group with C(9) [C(9)···S(2) (1 + x, y, z) 3.681(10) Å] to form a 3D hydrogen-bonded structure (see Figure S5 in the Supporting Information).

The hydrogen-bonding interactions in **5** are different to those in **4**. Thus, there are three intramolecular H-bonding interactions between the O atoms of NO_3^- anions and the methyl group with C(18) [C(18)···O(3) 3.361(11) Å] and the phenyl group with C(14) [C(14)···O(3) 3.430(8), C(14)···O(1) 3.259(9) Å]. In addition, there are further six intermolecular H-bonding interactions between the O atoms of NO_3^- anions and the methyl groups with C(7), C(9), and C(17) [C(7)···O(3) (1 + x, y, –1 + z) 3.442(9), C(9)···O(3) (2 – x, 1 – y, –z) 3.359(10), C(9)···O(2) (1 + x, y, –1 + z) 3.340(10), C(17)···O(2) (3/2 – x, 1/2 + y, 1/2 – z) 3.411(11) Å], and between the terminal Cl(1) atom and the phenyl group with C(5) [C(5)···Cl(1) (1/2 + x, 3/2 – y, –3/2 + z) 3.640(7) Å] and the methyl group with C(17) [C(17)···Cl(1) (3/2 – x, 1/2 + y, 1/2 – z) 3.715(7) Å]. These intra- and intermolecular H-bonding interactions lead to the formation of a 2D hydrogen-bonded network extending in the [101] plane (see Figure S7 in the Supporting Information).

Both **6** and **7** crystallize in the monoclinic space group $P2_1/n$ and the asymmetric unit contains half of a $[Hg(\mu\text{-}Tab)(Tab)X]_2^{2+}$ dication and one X^- anion [X = NO_2 (**6**), NO_3 (**7**)]. As **6** and **7** are structurally similar, only the perspective view of the dication in **6** is depicted in Figure 7. Each centrosymmetric dication consists of two $[Hg(Tab)_2X]^+$ [X = NO_2 (**6**); NO_3 (**7**)] cations that are interconnected through a pair of weak Hg–S bonds [3.222(3) Å for **6** and 3.273(3) Å for **7**]. The Hg···Hg contact in the dication is 4.143 Å for **6** and 4.172 Å for **7**, both of which are somewhat longer than those in **3**–**5**. The central Hg atom is coordinated by three S atoms of one terminal and two bridging Tab ligands and two O atoms of nitrite or nitrate anions and thus shows an "umbrella"-type coordination geometry. The shorter Hg–S bonds in **6** [av. 2.3528(12) Å] and **7** [av. 2.3732(11) Å] are normal when compared with those of the corresponding ones in **3**–**5**. The mean Hg–O bond length in **6** [2.663(6) Å] is in-between that of $[Hg(mtcb)_2]$ [av. 2.579(6) Å; mtcb = morpholinothiocarbonylbenzamide][18] and that of **7** [2.755(5) Å]. The linear configuration of the $[Hg(Tab)_2]^{2+}$ dication of **1** is retained in each $[Hg(Tab)_2X]^+$ [X = NO_2 (**6**); NO_3 (**7**)] cation.

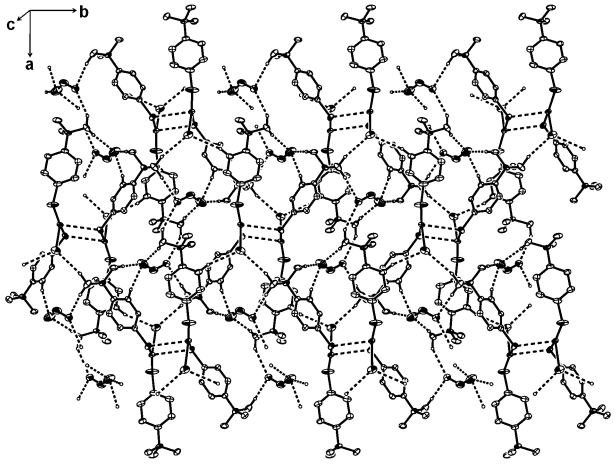

Figure 6. View of the two-dimensional network extending in the *ab* plane formed by intermolecular hydrogen-bonding interactions in **4**. All H atoms except those related to H-bonding interactions have been omitted for clarity.

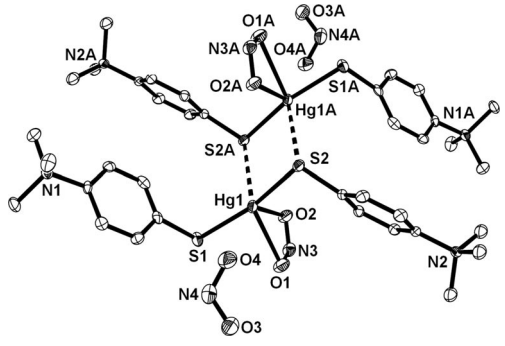

Figure 7. Perspective view of the molecular structure of **6** showing the atom labeling scheme and 50% thermal ellipsoids.

The hydrogen-bonding interactions in **6** are also complicated. Thus, there are two intermolecular H-bonding interactions between S(1) of the Tab ligand and the methyl groups with C(8) or C(16) [C(8)···S(1) (1 – *x*, 2 – *y*, 1 – *z*) 3.768(5), C(16)···S(1) (–1 + *x*, *y*, *z*) 3.784(5) Å], which form a chain running along the *a* axis. Adjacent chains are interlinked through five intermolecular H-bonding interactions between O atoms of the NO_2^- anions and the methyl groups with C(8), C(16), C(17), or C(18) [C(8)···O(4) (1/2 – *x*, 1/2 + *y*, 1/2 – *z*) 3.375(6), C(16)···O(4) (–1/2 + *x*, 3/2 – *y*, 1/2 + *z*) 3.486(6), C(17)···O(2) (–1/2 – *x*, –1/2 + *y*, 3/2 – *z*) 3.329(5), C(18)···O(2) (–1/2 – *x*, –1/2 + *y*, 3/2 – *z*) 3.331(5) Å] and the phenyl group with C(12) [C(12)···O(4) (–1/2 + *x*, 3/2 – *y*, 1/2 + *z*) 3.314(5) Å] to afford a 2D layer extending approximately in the *ab* plane (Figure S8 in the Supporting Information). Further three intermolecular H-bonding interactions between O atoms of NO_2^- anion in one layer and the methyl groups with C(7) and C(17) [C(7)···O(1) (1/2 + *x*, 3/2 – *y*, –1/2 + *z*) 3.392(6), C(17)···O3 (–*x*, 1 – *y*, 1 – *z*) 3.393(6) Å] or the phenyl group with C(3) [C(3)···O(1) (1/2 + *x*, 3/2 – *y*, – 1/2 + *z*) 3.219(5) Å] in an adjacent layer complete a 3D hydrogen-bonded network (see Figure S9 in the Supporting Information).

In the case of **7**, three intramolecular H-bonding interactions between the O atoms in NO_3^- anions with H atoms of the methyl groups [C(16)···O(5) 3.419(5) Å] and phenyl groups [C(15)···O(2) 3.461(4), C(14)···O(5) 3.491(5) Å], along with three intermolecular H-bonding interactions between O atoms of NO_3^- anions and the phenyl group with C(5) [C(5)···O(1) (–1/2 + *x*, 1/2 – *y*, 1/2 – *z*) 3.264(4) Å] and the methyl group with C(7) [C(7)···O(1) (–1/2 + *x*, 1/2 – *y*, 1/2 – *z*) 3.838(5) Å] give rise to a chain structure (Figure S11 in the Supporting Information). Furthermore, adjacent chains are connected via another four intermolecular H-bonding interactions between the O atoms of NO_3^- anions and the methyl groups with C(18), C(8), and C(9) [C(18)···O(2) (3/2 – *x*, 1/2 + *y*, 1/2 – *z*) 3.318(4), C(9)···O(5) (1 – *x*, –*y*, 1 – *z*) 3.342(5), C(8)···O(4) (–1 + *x*, *y*, 1 + *z*) 3.458(5), C(8)···O(4) (1 – *x*, –*y*, 1 – *z*) 3.475(5) Å] to form a two-dimensional hydrogen-bonded network extending in the [101] plane (see Figure S12 in the Supporting Information).

As indicated in Table 1, the mean Hg–S bond length of 2.3576(17) Å in **2** (three-coordinate) is slightly longer than that in **1** [2.331(4) Å, two-coordinate] but significantly shorter than those in four-coordinate [2.617(2) Å in **3**, 2.602(2) Å in **4**, 2.573(3) Å in **5**] and five-coordinate Hg^{II}/Tab compounds [2.643(3) Å in **6** and 2.653(3) Å in **7**]. Thus, the Hg–S bond lengths in **1**–**7** depend on the coordination geometries around the Hg centers and their coordination numbers, which is similar to the work reported recently.[19]

Conclusions

We have demonstrated the interesting reactivity of a precursor complex **1** towards the naturally occurring inorganic anions Cl^-, NO_2^-, and NO_3^- and successful isolation of a family of six new mecury(II) complexes (**2**–**7**) consisting of these anions. According to X-ray analysis, the structures of the cations in **2**–**7** are different from that of **1** when these anions coordinate to the Hg^{II} center of **1**. Thus, the linear Hg^{II} atom of **1** is converted into a T-shaped (**2**), tetrahedral (**3**–**5**) or "umbrella"-shaped (**6**–**7**) coordination geometry. It should be noted that the coordination geometry at the Hg centre and its coordination number strongly affect the Hg–S bond lengths of **1**–**7**. Compared with those of **1**, the two $^-SC_6H_4NMe_3^+$ groups of each $[Hg(Tab)_2Cl]^+$ cation in **4**, **6**, and **7** retain their original orientations while those of **2**, **3**·H_2O, and **5** are oriented in the same directions, which imply that in the latter case one of the two $^-SC_6H_4NMe_3^+$ groups of **1** are rotated during the reaction. Moreover, crystals of **2**–**7** show abundant intra- and intermolecular H-bonding interactions between the inorganic anions (Cl^-, NO_2^-, NO_3^-) and the methyl or phenyl groups of the Tab ligands, which lead to the formation of intriguing 2D or 3D hydrogen-bonded networks. We are currently extending this work by investigating the reactivity of the Hg^{II} center of **1** toward carboxylates and N-containing heterocyclic compounds encountered in nature.

Experimental Section

General Remarks: Complex **1** was prepared according to the literature method.[7d] Other chemicals and reagents were obtained from commercial sources and used as received. All solvents were predried with activated molecular sieves and refluxed over the appropriate drying agents under argon. IR spectra were recorded with a Varian 1000 FT-IR spectrometer as KBr disks (4000–400 cm^{-1}). UV/Vis spectra were measured with a Varian 50 UV/Vis spectrophotometer. Elemental analyses for C, H and N were performed with a Carlo–Erba CHNO-S microanalyzer. ^1H NMR spectra were recorded at ambient temperature with a Varian UNITYplus-400 spectrometer. ^1H NMR chemical shifts are referenced to the deuterated dimethyl sulfoxide [$(CD_3)_2SO$] signal.

$[Hg(Tab)_2Cl](PF_6)$ (2): A solution of NaCl (0.058 g, 1 mmol) in MeOH (3 mL) and H_2O (1 mL) was added to a solution of **1** (0.825 g, 1 mmol) in MeCN (15 mL) and the resulting mixture was stirred for 0.5 h to form a colorless homogeneous solution. After filtration, diethyl ether (40 mL) was allowed to diffuse into the filtrate at ambient temperature for two weeks to form colorless needles of **2**, which were collected by filtration, washed by Et_2O, and dried in vacuo. Yield 0.66 g (93% based on Hg). $C_{18}H_{26}ClF_6HgN_2PS_2$ (715.56): calcd. C 30.21, H 3.66, N 3.92; found C 30.42, H 3.73, N 3.89. IR (KBr disc): $\tilde{\nu}$ = 1584 (w), 1491 (s), 1415 (m), 1127 (m), 1011 (m), 956 (m), 839 (s), 744 (w), 558 (s) cm^{-1}. ^1H NMR [400 MHz, $(CD_3)_2SO$]: δ = 7.57–7.68 (m, 4 H, Ph), 3.32 (s, 9 H, NMe_3) ppm.

$[Hg(\mu\text{-}Tab)(Tab)Cl]_2Cl_2\cdot H_2O$ (3·H_2O): A solution of NaCl (0.116 g, 2 mmol) in MeOH (5 mL) and H_2O (2 mL) was added to a solution of **1** (0.825 g, 1 mmol) in MeCN (15 mL) and the resulting mixture was stirred for 0.5 h to form a colorless homogeneous solution. After filtration, slow evaporation of the solvents from the filtrate overnight afforded colorless blocks of **3**·H_2O. Yield 0.51 g (82% based on Hg). $C_{36}H_{54}Cl_4Hg_2N_4OS_4$ (1230.1): calcd. C 35.15, H 4.42, N 4.55; found C 35.50, H 4.37, N 4.58. IR (KBr disc): $\tilde{\nu}$ = 1582 (m), 1491 (s), 1416 (m), 1129 (s), 1011 (w), 957 (w),

849 (w), 744 (w), 558(w) cm^{-1}. ^1H NMR [400 MHz, $(CD_3)_2SO$]: δ = 7.58–7.75 (m, 4 H, Ph), 3.43 (s, 9 H, NMe_3) ppm.

$[Hg(\mu\text{-}Tab)(Tab)Cl]_2(NO_2)_2$ (4): A mixture of NaCl (0.058 g, 1 mmol) and $NaNO_2$ (0.069 g, 1 mmol) in MeOH (5 mL) and H_2O (2 mL) was added to a solution of **1** (0.825 g, 1 mmol) in MeCN (15 mL) and the resulting mixture was stirred for 0.5 h to form a homogeneous solution. Slow evaporation of the solvents from the filtrate afforded colorless blocks of **4** overnight. Yield 0.49 g (79% based on Hg). $C_{36}H_{52}Cl_2Hg_2N_6O_4S_4$ (1233.2): calcd. C 35.06, H 4.25, N 6.81; found C 35.13, H 4.41, N 6.56. IR (KBr disc): $\tilde{\nu}$ = 1582 (w), 1490 (s), 1412 (m), 1273 (s), 1219 (s), 1127 (w), 1011 (m), 957 (m), 849 (m), 749 (w), 558 (m) cm^{-1}. ^1H NMR [400 MHz, $(CD_3)_2SO$]: δ = 7.38–7.65 (m, 4 H, Ph), 3.39 (s, 9 H, NMe_3) ppm.

$[Hg(\mu\text{-}Tab)(Tab)Cl]_2(NO_3)_2$ (5): Compound **5** (colorless crystals) was prepared as above starting from **1** (0.825 g, 1 mmol), NaCl (0.058 g, 1 mmol), and $NaNO_3$ (0.085 g, 1 mmol). Yield 0.47 g (74% based on Hg). $C_{36}H_{52}Cl_2Hg_2N_6O_6S_4$ (1265.2): calcd. C 34.18, H 4.14, N 6.64; found C 34.03, H 4.41, N 6.56. IR (KBr disc): $\tilde{\nu}$ = 1582 (m), 1490 (s), 1382 (s), 1281 (m), 1242 (m), 1119 (m), 1088 (m), 1011 (w), 957 (s), 848 (w), 745 (w), 557 (w) cm^{-1}. ^1H NMR [400 MHz, $(CD_3)_2SO$]: δ = 7.37–7.63 (m, 4 H, Ph), 3.40 (s, 9 H, NMe_3) ppm.

$[Hg(\mu\text{-}Tab)(Tab)(NO_2)]_2(NO_2)_2$ (6): A solution of $NaNO_2$ (0.14 g, 2 mmol) in MeOH (3 mL) and H_2O (2 mL) was added to a stirred solution of **1** (0.825 g, 1 mmol) in dmf (3 mL) and the resulting solution was stirred for 0.5 h. A similar work-up to that used in the isolation of **3**·H_2O produced colorless blocks of **6**. Yield 0.45 g (72% based on Hg). $C_{36}H_{52}Hg_2N_8O_8S_4$ (1254.3): calcd. C 34.47, H 4.18, N 8.93; found C 34.33, H 4.41, N 8.74. IR (KBr disc): 1581 (m), 1489 (s), 1417 (w), 1270 (br., s), 1210 (br., s), 1125 (m), 1008 (m), 960 (w), 848 (m), 746 (w), 556 (w) cm^{-1}. ^1H NMR [400 MHz, $(CD_3)_2SO$]: δ = 7.57 –7.66 (m, 4 H, Ph), 3.40 (s, 9 H, NMe_3) ppm.

$[Hg(\mu\text{-}Tab)(Tab)(NO_3)]_2(NO_3)_2$ (7): Compound **7** (colorless crystals) was prepared as above starting from **1** (0.825 g, 1 mmol) and $NaNO_3$ (0.17 g, 1 mmol). Yield 0.48 g (73% based on Hg). $C_{36}H_{52}Hg_2N_8O_{12}S_4$ (1318.3): calcd. C 32.80, H 3.98, N 8.50; found C 32.53, H 4.15, N 8.41. IR (KBr disc): $\tilde{\nu}$ = 1580 (w), 1488 (s), 1384 (br., s), 1324 (br., s), 1123 (m), 1010 (w), 957 (m), 847 (m), 746 (w), 558 (w) cm^{-1}. ^1H NMR [400 MHz, $(CD_3)_2SO$]: δ = 7.55–7.69 (m, 4 H, Ph), 3.37 (s, 9 H, NMe_3) ppm.

X-ray Structure Determinations: All measurements were performed with a Rigaku Mercury CCD X-ray diffractometer by using graphite-monochromated Mo-K_α (λ = 0.71070 Å). Single crystals of **2**–**7** suitable for X-ray analysis were obtained directly from the above preparations. These crystals were mounted on glass fibers and cooled in a liquid nitrogen stream to 153 K for **2**, **3**·H_2O, and **5**–**7** and 133 K for **4**. Diffraction data were collected in ω mode with a detector-to-crystal distance of 35 mm. Cell parameters were refined by using the program Crystalclear (Rigaku and MSc, Ver. 1.3, 2001) on all observed reflections between 6.1° and 50.7° for **2** and **3**·H_2O, 6.2° and 50.7° for **4**–**6**, and 6.3° and 50.70° for **7**. The collected data were reduced by using the program CrystalClear (Rigaku and MSc, Ver. 1.3, 2001), and an absorption correction (multi-scan) was applied, which resulted in transmission factors ranging from 0.433 to 0.573 for **2**, 0.206 to 0.230 for **3**·H_2O, 0.091 to 0.156 for **4** and 0.297 to 0.382 for **5**, 0.264 to 0.313 for **6** and 0.094 to 0.244 for **7**. The reflection data were also corrected for Lorentz and polarization effects.

The crystal structures of **2**–**7** were solved by direct methods and refined on F^2 by full-matrix least-squares using anisotropic displacement parameters for all non-hydrogen atoms.[20] The Hg atoms in **4** were found to be split into two sites with an occupancy ratio of 0.6875/0.3125 for Hg(1)/Hg(1A). The Hg and S atoms in **5** were split into two sites with an occupancy ratio of 0.526/0.474 for Hg(1)/Hg(1A) and S(1)/S(1A). The hydrogen atoms of the water

Table 2. Crystallographic data and structure refinement for **2**–**7**.

Compound	**2**	**3**·H_2O	**4**	**5**	**6**	**7**
Molecular formula	$C_{18}H_{26}ClF_6HgN_2PS_2$	$C_{36}H_{54}Cl_4Hg_2N_4OS_4$	$C_{36}H_{52}Cl_2Hg_2N_6O_4S_4$	$C_{36}H_{52}Cl_2Hg_2N_6O_6S_4$	$C_{36}H_{52}Hg_2N_8O_8S_4$	$C_{18}H_{26}HgN_4O_6S_2$
Formula weight	715.56	1230.05	1233.2	1265.16	1254.32	1318.32
Crystal system	monoclinic	monoclinic	monoclinic	monoclinic	monoclinic	monoclinic
Space group	$P2_1/c$	Pn	$P2_1/c$	$P2_1/n$	$P2_1/n$	$P2_1/n$
Size	0.24×0.10×0.08	0.22×0.20×0.19	0.33×0.30×0.25	0.36×0.14×0.13	0.25×0.16×0.16	0.45×0.30×0.20
a [Å]	10.179(2)	11.4277(11)	11.446(2)	11.637(2)	11.388(2)	11.166(2)
b [Å]	26.448(5)	14.2575(13)	14.249(3)	14.168(3)	14.619(3)	14.623(3)
c [Å]	8.6864(17)	13.3267(13)	16.705(5)	13.190(3)	13.207(5)	13.914(3)
β [°]	96.19(3)	94.970(2)	127.92(2)	95.21(3)	95.76(3)	94.78(3)
V [Å^3]	2324.9(8)	2163.2(4)	2149.3(10)	2165.7(8)	2187.6(8)	2264.0(8)
Z	4	2	2	2	4	4
T [K]	153(2)	153(2)	153(2)	153(2)	153(2)	153(2)
$D_{calcd.}$ [g cm^{-3}]	2.044	1.888	1.906	1.940	1.904	1.934
λ (Mo-K_α) [Å]	0.71073	0.71070	0.71073	0.71073	0.71073	0.71073
μ [cm^{-1}]	70.41	42.53	74.98	74.47	72.58	70.25
$2\theta_{max}$ [°]	55.7	50.6	50.7	50.7	50.7	50.7
Total reflections	22480	21159	20569	20230	20569	21688
Unique reflections	4258 (R_{int} = 0.083)	7107 (R_{int} = 0.028)	3917 (R_{int} = 0.0406)	3949 (R_{int} = 0.0888)	4002 (R_{int} = 0.0381)	4140 (R_{int} = 0.0345)
Observations	3678 [$I > 2.00\sigma(I)$]	6902 [$I > 2.00\sigma(I)$]	3593 [$I > 2.00\sigma(I)$]	3331 [$I > 2.00\sigma(I)$]	3641 [$I > 2.00\sigma(I)$]	3922 [$I > 2.00\sigma(I)$]
Parameters	287	434	259	278	256	286
R[a]	0.0637	0.0218	0.0551	0.0442	0.0273	0.0231
wR[b]	0.1046	0.0433	0.1171	0.0848	0.0499	0.0505
GOF[c]	1.102	1.062	1.104	1.072	1.185	1.182
$\Delta\rho_{max}$ [e Å^{-3}]	1.335	0.860	1.156	0.510	1.073	0.642
$\Delta\rho_{min}$ [e Å^{-3}]	–1.117	–0.702	–1.109	–0.634	–0.689	–0.855

[a] $R = \Sigma||F_o| - |F_c||/\Sigma|F_o|$. [b] $wR = \{\Sigma w(F_o^2 - F_c^2)^2/\Sigma w(F_o^2)^2\}^{1/2}$. [c] GOF = $\{\Sigma[w\{(F_o^2 - F_c^2)^2\}/(n - p)]\}^{1/2}$, where n is the number of reflections and p the total number of parameters refined.

molecule in **3**·H_2O were located from Fourier maps. All other hydrogen atoms were placed in geometrically idealized positions (C–H 0.98 Å for methyl groups; C–H 0.95 Å for phenyl groups) and constrained to ride on their parent atoms with $U_{iso}(H) = 1.2U_{eq}(C)$ for phenyl groups and $U_{iso}(H) = 1.5U_{eq}(C)$ for methyl groups. Important crystal data and collection and refinement parameters for **2**–**7** are summarized in Table 2.

CCDC-666263 (for **2**), -666264 (for **3**·H_2O), -666265 (for **4**), -666266 (for **5**), -666267 (for **6**), -666268 (for **7**) contain the supplementary crystallographic data for this paper. These data can be obtained free of charge from The Cambridge Crystallographic Data Center via http://www.ccdc.cam.ac.uk/data_request/cif

Supporting Information (see also the footnote on the first page of this article): Twelve figures with different stereoviews of the network structures of compounds **2**–**7**.

Acknowledgments

This work was supported financially by the National Natural Science Foundation of China (grant no. 20525101), the Specialized Research Fund for the Doctoral Program of Higher Education (grant no. 20050285004), the State Key Laboratory of Coordination Chemistry of Nanjing University, the Qin-Lan Project of Jiangsu Province, and the Program for Innovative Research Team of Soochow University in China. We are also grateful to the reviewers for their helpful suggestions.

[1] G. Henkel, B. Krebs, *Chem. Rev.* **2004**, *104*, 801–824.
[2] P. J. Blower, J. R. Dilworth, *Coord. Chem. Rev.* **1987**, *76*, 121–185.
[3] a) J. Chan, Z. Y. Huang, M. E. Merrifield, M. T. Salgado, M. J. Stillman, *Coord. Chem. Rev.* **2002**, *233–234*, 319–339; b) A. Leiva-Presa, M. Capdevila, P. Gonzalez-Duarte, *Eur. J. Biochem.* **2004**, *271*, 4872–4880; c) I. G. Dance, *Polyhedron* **1986**, *5*, 1037–1104.
[4] *Metallothioneins*, in *Synthesis, Structure and Properties of Metallothioneins, Phytochelatins and Metal-Thiolate Complexes* (Eds.: M. J. Stillman, C. F. Shaw, K. T. Suzuki), John Wiley & Sons, New York, **1992**.
[5] a) W. H. Lu, M. J. Stillman, *J. Am. Chem. Soc.* **1993**, *115*, 3291–3299; b) L. M. Shewchuk, G. L. Verdine, H. Nash, C. T. Walsh, *Biochemistry* **1989**, *28*, 6140–6145; c) S. P. Watton, J. G. Wright, F. M. MacDonnell, J. W. Bryson, M. Sabat, T. V. O'Halloran, *J. Am. Chem. Soc.* **1990**, *112*, 2824–2826; d) J. D. Helmann, B. T. Ballard, C. T. Walsh, *Science* **1990**, *247*, 946–948.
[6] a) W. H. Lu, A. J. Zelazowski, M. J. Stillman, *Inorg. Chem.* **1993**, *32*, 919–926; b) W. Cai, M. J. Stillman, *J. Am. Chem. Soc.* **1988**, *110*, 7872–7873; c) D. T. Jiang, S. M. Heald, T. K. Sham, M. J. Stillman, *J. Am. Chem. Soc.* **1994**, *116*, 11004–11013.
[7] a) J. X. Chen, Q. F. Xu, Y. Xu, Y. Zhang, Z. N. Chen, J. P. Lang, *Eur. J. Inorg. Chem.* **2004**, 4247–4252; b) J. X. Chen, Q. F. Xu, Y. Zhang, Z. N. Chen, J. P. Lang, *J. Organomet. Chem.* **2004**, *689*, 1071–1077; c) J. X. Chen, W. H. Zhang, X. Y. Tang, Z. G. Ren, H. X. Li, Y. Zhang, J. P. Lang, *Inorg. Chem.* **2006**, *45*, 7671–7680; d) J. X. Chen, W. H. Zhang, X. Y. Tang, Z. G. Ren, Y. Zhang, J. P. Lang, *Inorg. Chem.* **2006**, *45*, 2568–2580.
[8] a) K. Nakamoto, *Infrared and Raman Spectra of Inorganic and Coordination Compounds*, *Part B: Applications in Coordination, Organometallic, and Bioinorganic Chemistry* (5th ed.), John Wiley & Sons, New York, **1997**, pp. 51–52; b) S. Ferrer, R. Ballesteros, A. Sambartolom, M. Gonzalez, G. Alzuet, J. Borras, M. Liu, *J. Inorg. Biochem.* **2004**, *98*, 1436–1446.
[9] a) A. Schaffer, K. Williman, H. Willner, *J. Inorg. Biochem.* **1989**, *36*, 186–192; b) M. S. Bharara, T. H. Bui, S. Parkin, D. A. Atwood, *Inorg. Chem.* **2005**, *44*, 5753–5760; c) M. S. Bharara, S. Parkin, D. A. Atwood, *Inorg. Chem.* **2006**, *45*, 2112–2118.
[10] R. Tamilarasan, D. R. McMillin, *Inorg. Chem.* **1986**, *25*, 2037–2040.
[11] a) M. Beltramine, K. Lerch, M. Vasak, *Biochemistry* **1984**, *23*, 3422–3427; b) B. A. Johnson, I. M. Armitage, *Inorg. Chem.* **1987**, *26*, 3139–3144.
[12] N. J. Taylor, A. J. Carty, *J. Am. Chem. Soc.* **1977**, *99*, 6143–6145.
[13] A. J. Carty, N. J. Taylor, *J. Chem. Soc., Chem. Commun.* **1976**, 214–216.
[14] C. M. V. Stalhandske, I. Persson, M. Sandstrom, M. Aberg, *Inorg. Chem.* **1997**, *36*, 4945–4953.
[15] G. Faraglia, R. Graziani, L. Sindellari, E. Forsellini, U. Casellato, *Inorg. Chim. Acta* **1982**, *58*, 167–172.
[16] P. D. Brotherton, P. C. Healy, C. L. Raston, A. H. White, *J. Chem. Soc., Dalton Trans.* **1973**, 334–336.
[17] G. A. Bowmaker, I. G. Dance, B. C. Dobson, D. A. Rogers, *Aust. J. Chem.* **1984**, *37*, 1607–1618.
[18] W. Q. Zhou, W. Yang, L. H. Qiu, Y. Zhang, Z. Y. Yu, *J. Mol. Struct.* **2005**, *749*, 89–95.
[19] A. Manceau, K. L. Nagy, *Dalton Trans.* **2008** (DOI: 10.1039/b718372k).
[20] G. M. Sheldrick, *SHELXS-97* and *SHELXL-97*, Program for the refinement of crystal structures, University of Göttingen, Germany, **1997**.

Received: January 31, 2008
Published Online: April 25, 2008

